Modeling of InP HBTs in Transferred-Substrate Technology for Millimeter-Wave Applications

Tom K. Johansen[1], Matthias Rudolph[2,3], Thomas Jensen[3], Tomas Kraemer[3], Nils Weimann[3], Frank Schnieder[3], Viktor Krozer[3], and Wolfgang Heinrich[3]
[1]Technical University of Denmark, Department of Electrical Engineering, DK-2800 Kgs. Lyngby, Denmark
Email: tkj@elektro.dtu.dk
[2]Brandenburg University of Technology, D-03046 Cottbus, Germany
[3]Ferdinand-Braun-Institut (FBH), Leibniz-Institut für Höchstfrequenztechnik, D-12489 Berlin, Germany

***Abstract*—In this paper, the modeling of InP heterojunction bipolar transistors (HBTs) in transferred substrate (TS) technology is investigated. At first, a direct parameter extraction methodology dedicated to III-V based HBTs is employed to determine the small-signal equivalent circuit parameters from measured S-parameters. It is shown that the model prediction of measured S-parameters can be improved in the millimeter-wave frequency range by augmenting the small-signal model with a description of AC current crowding. The extracted elements of the small-signal model structure are employed as a starting point for the extraction of a large-signal model. The developed large-signal model for the TS-HBTs accurately predicts the DC over temperature and small-signal performance over bias as well as the large-signal performance at millimeter-wave frequencies (77 GHz).**

***Index Terms*—Heterojunction bipolar transistor (HBT), equivalent circuit modeling, parameter extraction, InP, transferred substrate.**

I. INTRODUCTION

InP-based HBTs in transferred substrate technology have demonstrated excellent high frequency operation with simultaneous high output power densities [1]. Compared with a conventional triple mesa HBT, the transferred substrate technology allows a reduction of the extrinsic parasitic capacitance between the base and collector semiconductor regions of the HBT device. This leads to devices demonstrating extremely high frequency operation with potential for active electronics in the sub-THz (0.1-1 THz) frequency range [2].

From a modeling point of view the TS-HBT devices are expected to behave quite similar to other III-V based HBTs. In HBTs based on III-V materials the dependence of the electron velocity on electrical field leads to a complicated bias dependence for the cut-off frequency f_t and base-collector capacitance C_{bc}. The cut-off frequency is determined from the total emitter-collector delay in the device and is dominated by the collector transit time. Large-signal models for III-V based HBTs, such as the UCSD HBT model, FBH HBT model, and the Agilent HBT model mainly differ in their way of implementing electron velocity modulation effects [4]. Another effect often seen in InP-based double HBTs is related to the formation of a barrier for electron flow at the base-collector heterojunction at high collector current levels (collector blocking). Collector blocking manifests itself

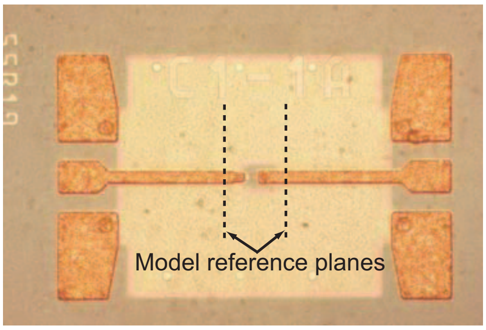

Fig. 1. Microphotograph of on-wafer test-structure for single-finger TS-HBT device with $0.8 \times 6\text{-}\mu m^2$ emitter area showing reference planes for model extraction.

in the output characteristic as a soft transition between the saturation region and the forward active region (similar to quasi-saturation). For this reason it is sometimes referred to as the ”soft-knee” effect. The UCSD and Agilent HBT models both include parameters to model the ”soft-knee” effect but it is not yet implemented in the FBH model. For some III-V based HBTs it has proven necessary to augment the small-signal equivalent circuit model with a capacitor C_{bi} in shunt with the intrinsic base resistance R_{bi} to represent AC-current crowding [5]. This effect has not yet been implemented in any of the large-signal HBT models mentioned above and it remains questionable whether the effect is noticeable in TS-HBTs.

In this paper, the small-signal structure for TS-HBTs is discussed and a direct parameter extraction methodology is outlined which allows the determination of the extrinsic base and emitter access impedances of the small-signal equivalent circuit model without relying on the ”open-collector” method [6]. After the determination of the small-signal equivalent circuit model the ability of the FBH HBT model to predict the large-signal performance of TS-HBTs with good accuracy at millimeter-wave frequencies is demonstrated for the first time.

II. TEST-STRUCTURE LAYOUT AND DE-EMBEDDING

The TS-HBT devices considered in this paper have been developed at the Ferdinand-Braun-Institute (FBH) and features

f_t and f_{max} values above 400 GHz [3]. Fig. 1 shows a microphotograph of the on-wafer test-structure for a single-finger TS-HBT device with 0.8×6-μm^2 emitter area. Part of the ground plane underneath the base terminal line is removed for lower parasitic capacitance but leads to an increase in base access inductance as will be shown later. As a model to be used for circuit design should represent the integrated device the reference planes for model extraction are located at the boundary of the device layout cell. The de-embedding of the pads and access micro-strip lines is performed in two steps: At first, an equivalent circuit model for an 420 μm long microstrip line connected with pads at both ends is developed from measured S-parameters. Next the influence from the pads and access microstrip lines is removed from the measured S-parameters of the TS-HBT device by straightforward manipulations.

III. Small-Signal Equivalent Circuit Modeling

A. Small-Signal Model Structure

The small-signal model structure proposed for the TS-HBT devices considered in this work is shown in Fig. 2. A hybrid-π small-signal equivalent circuit topology is chosen as it corresponds well to the linearized circuit arising from most large-signal models. A parasitic collector-emitter overlap capacitance C_{pc} is included at the output of the small-signal equivalent circuit model. Due to the opening of the ground plane underneath the base terminal any overlap capacitances between the base-emitter terminals are expected to be of small value. It can therefore be absorbed into the much larger internal base-emitter capacitance C_{be} without any consequence for the model accuracy. In InP-based TS-HBTs a significant part of the total transit-time stems from the collector region and may lead to transcapacitances in a small-signal description of the device [4]. In the hybrid-π equivalent circuit model the effect of transcapacitances can be modeled as an equivalent time-delay τ on the transconductance as shown in Fig. 2. For some III-V based HBTs the effect of AC-current crowding is noticeable and needs to be modeled [5]. In this case the small-signal model structure can be augmented with a capacitance C_{bi} in shunt with the intrinsic base resistance R_{bi} as indicated in Fig. 2.

B. Direct Parameter Extraction Methodology

The extraction of the elements of the small-signal equivalent circuit model follows an analytical procedure based on the two-port parameters measured in cut-off, open-collector, and forward active biasing modes. Starting from the collector side, the collector-emitter overlap capacitance C_{pc} is first extracted from cut-off mode Y-parameters. This is followed by the extraction of the collector resistance R_c and collector inductance L_c from Z-parameters measured under the open-collector condition. The open-collector method [6] is the standard way to extract also the access base and emitter impedances of HBTs. The method, however, is complicated by a distributed diode between the base and collector. This leads to an underestimation of the external base resistance R_b and an overestimation of the emitter resistance R_e as discussed in

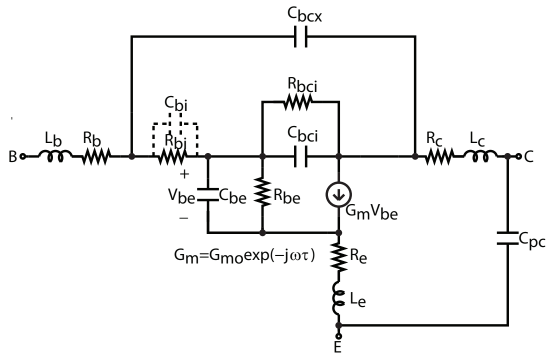

Fig. 2. Small-signal equivalent circuit model for the TS InP HBT device. The capacitance C_{bi} is included in the augmented small-signal equivalent circuit model.

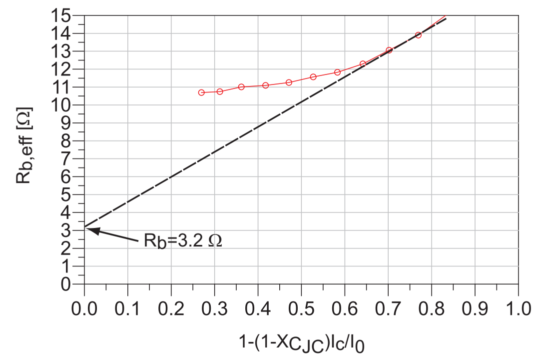

Fig. 3. Effective base resistance plotted versus $1-(1-X_{Cjc})I_c/I_0$ for external base resistance extraction. The dashed line is the linear extrapolation using parameters $X_{Cjc} = 0.6$ and $I_0 = 25.0$ mA.

[7]. Furthermore, to assure proper convergence of the extracted elements, very large base currents are often required with high risk for device damage. In [8] an alternative approach based on two-port parameters measured in the forward-active mode was proposed. The method exploits the physical behavior of the base-collector capacitance found in III-V based HBTs:

$$C_{bc} = C_{bc0}\left(1 - \frac{I_c}{I_0}\left[1 - \frac{I_c}{I_{tc}}\right]\right) \tag{1}$$

where C_{bc0} is the total base-collector capacitance at zero current, I_0 is a characteristic current describing the electron velocity modulation effect due to electric field in the collector, and I_{tc} is another characteristic current describing the response of the electric field to current flow in the collector. Based on the small-signal equivalent circuit diagram in Fig. 2 an effective base resistance can be defined at lower frequencies, $\omega^2 C_{bc}^2 R_{bi}^2 X^2 (1-X)^2 \ll 1$, as:

$$R_{b,eff} = \Re(Z_{11} - Z_{12}) \approx R_b + X(I_c) R_{bi} \tag{2}$$

where the current dependent distribution factor, $X(I_c)$, for the base-collector capacitance is approximated as

$$X(I_c) = \frac{C_{bci}}{C_{bc}} \approx X_{Cjc}\left[1 - (1 - X_{Cjc})\frac{I_c}{I_0}\right] \tag{3}$$

for $I_c/I_0 \ll 1$ and $X_{Cjc} = C_{bci0}/C_{bc0}$ at zero current has been introduced. The distribution factor at zero current can

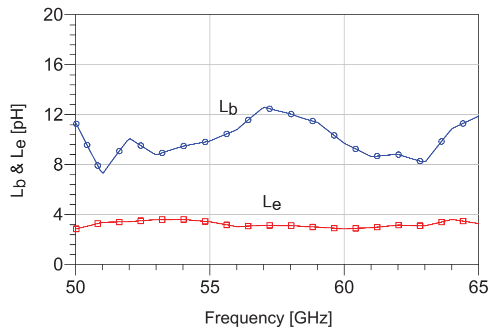

Fig. 4. Extraction of base and emitter inductances in the frequency range from 50 GHz to 65 GHz.

be extracted from cut-off mode measurements as described in [8]. The extracted effective base resistance values extrapolated to the collector current $I_c = I_0/(1 - X_{Cjc})$ are observed to reduce to the extrinsic base resistance R_b as the linear approximation for $X(I_c)$ reaches zero at this point. Fig. 3 illustrates the external base resistance extraction method applied to the 0.8×6-μm^2 InP-based TS-HBT device. The emitter resistance R_e can also be extracted from the forward active mode using the method reported in [7].

Once the external resistances have been determined their influence is removed from the measured two-port parameters. The remaining elements of the small-signal equivalent circuit model can be determined, e.g. using the method reported in [9], by neglecting at first the influence of the base and emitter inductances. The base and emitter inductances are then extracted using the elements determined in the previous step as follows [10]

$$L_b = \frac{1}{\omega}\Im\left(Z_{11} - Z_{12} - \frac{R_{bi}Z_{bcx}}{R_{bi} + Z_{bci} + Z_{bcx}}\right) \quad (4)$$

and

$$L_e = \frac{1}{\omega}\Im\left(Z_{12} - \frac{Z_{be}}{1 + G_m Z_{be}} - \frac{R_{bi}Z_{bci}}{(R_{bi} + Z_{bci} + Z_{bcx})(1 + G_m Z_{be})}\right) \quad (5)$$

where $Z_{be} = R_{be}||\frac{1}{j\omega C_{be}}$, $Z_{bci} = R_{bci}||\frac{1}{j\omega C_{bci}}$, and $Z_{bcx} = \frac{1}{j\omega C_{bcx}}$. Fig. 4 illustrates the extraction of the base and emitter inductances applied to the 0.8×6-μm^2 InP-based TS-HBT device. The extraction is performed in the frequency range from 50 GHz to 65 GHz where the values shows the least dispersive behavior. A rather large base terminal inductance in the range of $8 - 12$ pH is extracted and has been verified by electromagnetic simulations. This is caused by the opening of the ground plane underneath the base line and is expected to have a significant influence on the performance of millimeter-wave circuits.

C. Extraction Results and Discussion

The small-signal equivalent circuit elements found from the direct parameter extraction methodology are provided in Table. I. Fig. 5 shows a comparison between the measured and simulated S-parameters for the 0.8×6-μm^2 TS-HBT device using these extracted elements. In general, the simulation with the small-signal model matches the measured data well but a slight deviation is observed in S_{11} above approximately 58 GHz. Whether this deviation is caused by the lack of AC current crowding modeling or by measurement inaccuracies is hard to assess. However, by assigning the physical plausible value of $(C_{be} + C_{bc})/5$ to the intrinsic base capacitance C_{bi} the match between measured data and simulated response is clearly improved as observed in Fig. 5.

TABLE I
SMALL-SIGNAL EQUIVALENT CIRCUIT ELEMENTS FOR 0.8×6-μm^2 TS-HBT DEVICE AT $V_{ce} = 1.6$ V; $I_c = 25.6$ MA. THE VALUE USED FOR C_{bi} IN THE AUGMENTED SMALL-SIGNAL EQUIVALENT CIRCUIT MODEL IS GIVEN IN PARENTHESIS.

C_{pc} $[fF]$	R_b $[\Omega]$	R_c $[\Omega]$	R_e $[\Omega]$	L_b $[pH]$	L_c $[pH]$	L_e $[pH]$	C_{bcx} $[fF]$
2.3	3.2	2.0	1.7	11.5	8.5	2.8	4.7
R_{bi} $[\Omega]$	C_{bi} $[fF]$	C_{be} $[fF]$	R_{be} $[\Omega]$	C_{bci} $[fF]$	R_{bci} $[k\Omega]$	G_{mo} $[mS]$	τ $[ps]$
18.1	0(49.0)	241.5	76.1	3.4	69.7	624	≈ 0

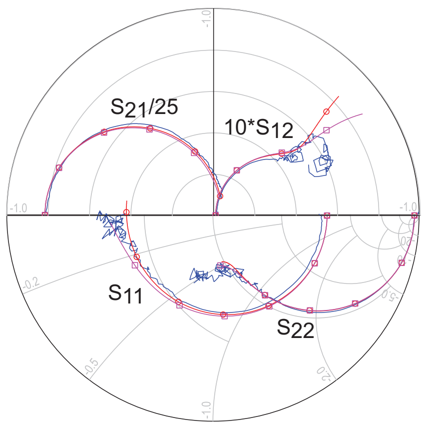

Fig. 5. S-parameters of 0.8×6-μm^2 TS-HBT device from 50 MHz-110 GHz. The figure compares measurements (solid line) with small-signal model response (solid line with circles), and augmented small-signal model response (solid line with squares). The bias point is at $V_{ce} = 1.6$; $I_c = 25.6$ mA.

IV. LARGE-SIGNAL MODELING

The large-signal modeling of the TS-HBTs is based on the FBH HBT model formulation. The FBH HBT model was originally developed for GaAs HBTs but should be versatile enough to model also InP-based HBTs [4]. After transferring the elements found from small-signal extraction to the large-signal model, the parameters affecting the DC and thermal characteristics of the device are determined. The forward output characteristics presented in Fig. 6 shows a quite different behavior compared to GaAs HBT devices. This is caused by an almost temperature independent forward current gain β_f typically found in InP-based HBTs. The forward output characteristic is modeled with reasonable accuracy even though the "soft-knee" effect caused by collector blocking (or quasi-saturation) is neglected so far by the FBH HBT

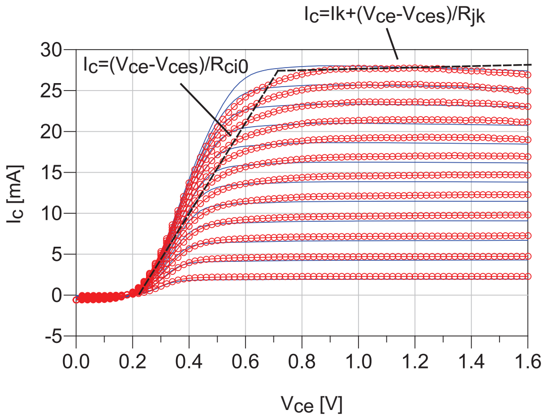

Fig. 6. Measured (solid line w. symbols) and modeled (solid line w.o. symbols) forward output characteristics. The base current is varied from 0.05 mA to 0.6 mA in steps of 0.05 mA. The dashed lines indicates chosen asymptotes for the onset of base push-out in the model.

model. As mentioned earlier, III-V based HBTs experience electron velocity modulating effects affecting both the base-collector capacitance and transit time. The FBH HBT model implements these effects through an unified collector charge [4]. The model parameters used to describe this collector charge are determined from the base-collector capacitance and cut-off frequency versus current extracted at different collector-emitter voltages. Despite the rather limited number of model parameters available to describe the collector charge it is found that the bias dependence of the small-signal parameters is well modeled. The onset of base push-out is controlled by the current I_{ck} with the asymptotes defined as $I_c = (V_{ce} - V_{ces})/R_{ci0}$ and $I_c = I_k + (V_{ce} - V_{ces})/R_{jk}$ where V_{ces}, R_{ci0}, I_k, and R_{jk} are model parameters. These asymptotes are indicated in the output characteristics of Fig. 6. As a possible work-around for the lack of "soft-knee" effect modeling we propose to adjust the model parameters R_{ci0} and V_{ces} to limit the RF signal swing into the "soft-knee" region. In this way, the model will limit any signal swing into this region through a sharp increase in the transit-time and base-collector capacitance.

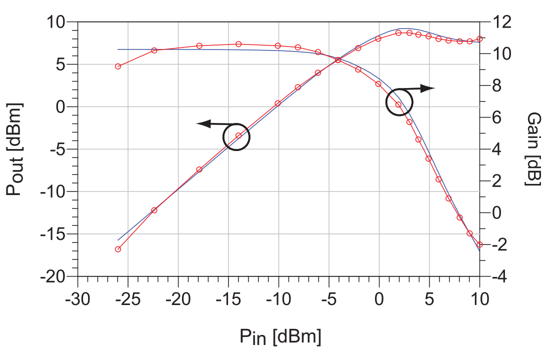

Fig. 7. Measured (solid line w. symbols) and simulated (solid line) large-signal performance at 77 GHz. The device is biased at $V_{ce} = 1.4$ V with a quiescent current of $I_{cq} = 22.7$ mA.

For verification of the developed TS-HBT large-signal model at millimeter-wave frequencies, the large-signal performance in a 50 Ω setup was measured using a 77 GHz Gunn source followed by a E-band attenuator. Input powers up to +10 dBm are possible with this setup. As seen in Fig. 7 the large-signal model is able to accurately predict the output power and gain compression characteristics even at the highest input power levels. This indicates that the base push-out parameter extraction approach proposed here for the FBH HBT large-signal model may be sufficient to model the "soft-knee" effect for practical purposes. Therefore, it does not seem strictly necessary to augment the model with a description of the "soft-knee" effect in order to better capture the characteristic of the InP-based TS-HBTs.

V. Conclusion

In this paper, the modeling of InP-based HBTs in transferred substrate technology was presented. The small-signal model structure augmented with an AC current crowding description improves the match to the measured S-parameters at highest frequencies. A developed large-signal model based on the FBH HBT model formulation without AC current crowding and "soft-knee" effects implemented provides good accuracy for the TS HBT devices, even at millimeter-wave frequencies.

References

[1] T. Jensen, T. Kraemer, T. Al-Sawaf, V. Krozer, W. Heinrich, and G. Traenkle, "Multifinger InP HBT's in Transferred-Substrate Technology for 100 GHz Power Amplifiers," in Proc. 7th European Microwave Integrated Circuits Conference, pp. 707-710, Amsterdam, The Netherlands, Nov., 2012.

[2] D. W. Scott, C. Monier, S. Wang, V. Radisic, P. Nguyen, A. Cavus, W. R. Deal, and A. G.-Aitken "InP HBT Transferred to Higher Thermal Conductivity Substrate," IEEE Trans. Electron Device Letters, Vol. 33, No. 4, pp. 507-509, April., 2012.

[3] T. Kraemer, M. Rudolph, F. J. Schmueckle, J. Wuerfl, and G. Traenkle, "InP DHBT Process in Transferred-Substrate Technology With f_t and f_{max} Over 400 GHz," IEEE Trans. Electron Devices, Vol. 56, No. 9, pp. 1897-1903, Sept., 2009.

[4] M. Rudolph, *Introduction to Modeling HBTs*. Artech House, Norwood, MA, 2006.

[5] L. Degachi, and F. M. Ghannouchi, "An Augmented Small-Signal HBT Model With Its Analytical Based Parameter Extraction Technique," IEEE Trans. Electron Devices, Vol. 55, No. 4, pp. 968-972, April 2008.

[6] Y. Gobert, P. J. Tasker and K. H. Bachem, "A physical, yet simple, small-signal equivalent circuit for the heterojunction bipolar transistor," IEEE Trans. Microwave Theory Tech., Vol. 45, No. 1, pp. 149-153, 1997.

[7] T. K. Johansen, V. Krozer, D. Hadziabdic, C. Jiang, A. Konczykowska, and J.-Y. Dupuy, "A novel method for HBT intrinsic collector resistance extraction from S-parameters," in Proc. of the Asia-Pacific Microwave Conference, pp. 1825-1828, Dec. 2007.

[8] T. K. Johansen, V. Krozer, V. Nodjiadjim, A. Konczykowska, J.-Y. Dupuy, and M. Riet, "Improved Extrinsic Base Resistance Extraction for Submicronmeter InP/InGaAs DHBT Models," IEEE Trans. Electron Devices, Vol. 58, No. 9, pp. 3004-3011, Sept. 2011.

[9] Y. Suh, J.-H. Shin, B. Kim, D. Heo, A. Radhavan, and J. Laskar, "Direct Extraction Method for Internal Equivalent Circuit Parameters of HBT Small-Signal Hybrid-Π Model," in IEEE MTT-S Digest, pp. 1403-1404, Jun. 2000.

[10] T. S. Horng, J. M. Wu, and H. H. Huang, "An Extrinsic-Inductance Independent Approach for Direct Extraction of HBT Intrinsic Circuit Parameters," in IEEE MTT-S Digest, pp. 1761-1764, Jun. 2001.